Population of intrinsic high spin states with the direct ^{116}Sn$(\alpha,p)^{119}$Sb reaction

P. A. Smith, R. A. Emigh, N. J. DiGiacomo, G. R. Smith, and R. J. Peterson
Nuclear Physics Laboratory, Department of Physics and Astrophysics, University of Colorado, Boulder, Colorado 80309
(Received 16 June 1978)

The ^{116}Sn$(\alpha,p)^{119}$Sb reaction at $E_\alpha = 35.6$ MeV has been used to locate previously unknown high spin states in ^{119}Sb. Cluster distorted-wave Born-approximation calculations have been employed to identify $L = 10$ ($J^\pi = 19/2^+, 21/2^+$) transfers to states at 4.120 ± 0.015 and 4.210 ± 0.015 MeV. A state located at $4.020 \pm .015$ MeV may be fit by either $L = 12$ or 14 distorted-wave Born-approximation curves. These high spin states are not members of the previously identified $K^\pi = 9/2^+$ rotational band. No evidence for population of this $9/2^+$ band was observed. Residual interaction matrix elements for the $(\nu h_{11/2}\pi s_{1/2})_{5^-,6^-}$ configurations have been deduced, assuming simple wave functions for the states populated by $L = 10$ transfers. The resulting matrix elements are in excellent agreement with the predictions of a δ force, as are other matrix elements extracted from the odd-odd Sb spectra.

[NUCLEAR REACTIONS ^{116}Sn$(\alpha,p)^{119}$Sb, separated isotope, measured $\sigma(E_p,\theta)$, cluster DWBA analysis, deduced residual interaction matrix elements.]

I. INTRODUCTION

The study of high spin states of nuclei remains one of the most active subjects in current nuclear physics research. In the case of spherical or nearly spherical nuclei, the intrinsic high spin states arise solely from the aligned coupling of a number of single nucleon angular momenta. The wave functions and excitation energies of these states should be well described by the shell model. The high spin states of ^{119}Sb, which are the subject of this paper, can be considered as a pair of $1h_{11/2}$ neutrons and a proton outside the $Z = 50$ closed shell. The energy of a $\frac{21}{2}^+$ state, described by the wave function $[\nu(h_{11/2})^2_{10}\pi s_{1/2}]_{21/2}$ with respect to the ^{116}Sn ground state, would then be

$$\epsilon_{21/2^+} = 2\epsilon^\nu_{11/2} + \epsilon^\pi_{1/2} + \langle\nu(h_{11/2})^2_{10}|V_{nn}|\nu(h_{11/2})^2_{10}\rangle$$
$$+2\left[[(21)(11)]^{1/2}\begin{pmatrix}11/2 & 11/2 & 10\\ 21/2 & 1/2 & 5\end{pmatrix}\right]^2\langle(\nu h_{11/2}\pi s_{1/2})_5|V_{np}|(\nu h_{11/2}\pi s_{1/2})_5\rangle$$
$$+2\left[[(21)(13)]^{1/2}\begin{pmatrix}11/2 & 11/2 & 10\\ 21/2 & 1/2 & 6\end{pmatrix}\right]^2\langle(\nu h_{11/2}\pi s_{1/2})_6|V_{np}|(\nu h_{11/2}\pi s_{1/2})_6\rangle\ ,$$

where $2\epsilon^\nu_{11/2} + \langle\nu(h_{11/2})^2_{10}|V_{nn}|\nu(h_{11/2})^2_{10}\rangle$ is the energy of the $(\nu h_{11/2})^2_{10^+}$ state in ^{118}Sn. In this simple model, mixing with other possible $\frac{21}{2}^+$ configurations involving $d_{3/2}$, $d_{5/2}$, and $g_{7/2}$ protons is neglected on the assumption that off-diagonal matrix elements are small compared to the diagonal terms, and the nucleons that comprise the ^{116}Sn ground state are presumed to be undisturbed by the addition of three nucleons. This model for the three-particle spectra near ^{208}Pb has proven to be highly successful in predicting the excitation energies of high spin states, including the $(i_{13/2})^{-3}_{33/2^+}$ state of ^{205}Pb,[1-5] although this is to be expected since ^{208}Pb is a good double shell closure. In this report we extend this model to the tin region where the protons comprise a closed shell but the neutrons are in the middle of a shell. A local shell model is used in the sense that a core of fixed, inactive nucleons is not assumed. Rather, we envision a model where the core is ^{116}Sn for the three-particle states in ^{119}Sb or the two-particle states in ^{118}Sb and ^{118}Sn, but would be ^{118}Sn if three-particle states in ^{121}Sb are considered.

The best way to populate the intrinsic high spin states of ^{119}Sb discussed above is to add the three nucleons directly onto the ^{116}Sn ground state via

the one-step direct $^{116}Sn(\alpha, p)^{119}Sb$ reaction. The angular momentum mismatch, which normally plagues distorted wave Born approximation (DWBA) calculations for multinucleon transfer reactions, works in our favor to enhance the cross sections of the high spin states. Furthermore, microscopic form factor calculations for the (α, p) reaction show that the stretched alignment produces a large form factor.[6] Indeed, some success has been obtained recently both detecting large angular momentum transfers with three-nucleon transfer and reproducing the angular distribution shapes with cluster model DWBA calculations.[7,8]

II. EXPERIMENT AND DATA

Spectra were obtained using the University of Colorado beam swinger and magnetic spectrometer with an incident beam of 35.6 MeV α particles. The target, which was made by evaporating the separated isotope onto a 20 $\mu g/cm^2$ carbon foil, was found to be approximately 250 $\mu g/cm^2$ thick by comparing elastic scattering data to an optical model calculation. The reaction products were detected in the spectrometer focal plane with a helical cathode proportional counter backed by a plastic scintillator. The protons were identified by their large scintillator signal relative to other particles. Further identification was done by requiring the scattered particles to have the proper time-of-flight relative to the cyclotron radio frequency. In addition, the reaction products were transversely deflected electrostatically[9] and the detector was positioned such that inelastic α particles did not strike the counter. Spectra were recorded for two excitation energy regions of 3 MeV each with approximately 1 MeV overlap. Sample spectra are shown in Fig. 1 where the energy resolution is about 50 keV full width at half maximum (FWHM).

The energy calibration for the levels below 3 MeV was obtained from known states of ^{119}Sb (Ref. 10) and the ^{15}N ground state, which came from the carbon backing on the target. The levels above 3 MeV proved difficult to calibrate because their Q values are more positive than the ground state Q values of heavier nuclei and negative enough to require knowledge of the states of nuclei in the mass 90 to 130 region 3 to 4 MeV in excitation. The most suitable Q values proved to be those of (α, p) on ^{13}C and ^{16}O. The procedure was to calibrate the small angle spectra with the $^{13}C(\alpha, p)^{16}N$ reaction and the ^{119}Sb states in the overlap region to determine the location of the 3.778 MeV state, which has a large cross section at forward angles. This state, the overlap region, the ^{15}N ground

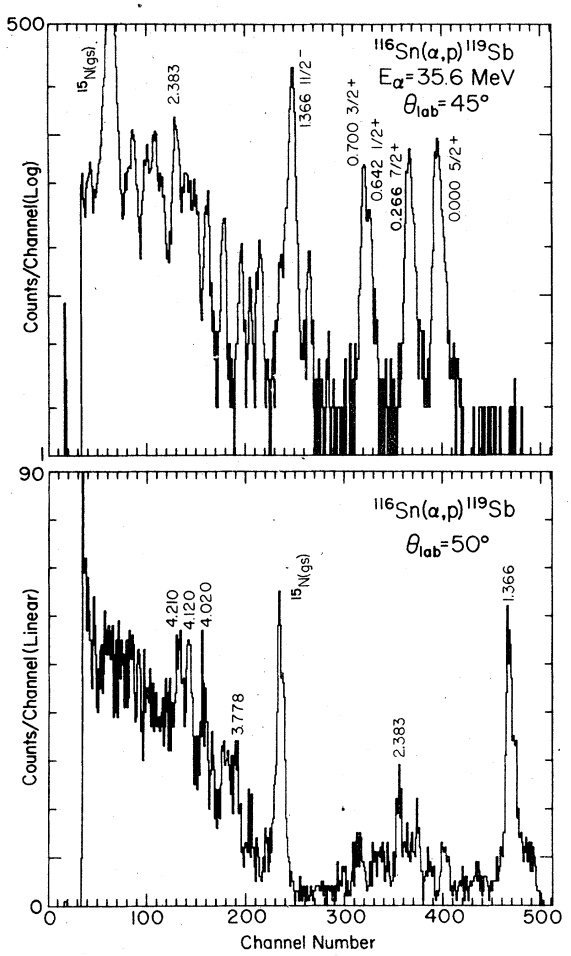

FIG. 1. Sample spectra of the $^{116}Sn(\alpha,p)^{119}Sb$ reaction at $E_\alpha = 35$ MeV. The angles and scales have been chosen to emphasize the peaks discussed in the text.

state, and the first two states of ^{19}F were then used to calibrate the spectra between 30° and 55°, where the candidates for high spin assignment were observed. The final excitation energies are given in Table I, along with the results of two γ-decay studies.[10,11]

The energies and spin assignments of the low-lying states observed in the (α, p) spectra are in excellent agreement with those observed in the $(p, n\gamma)$ experiment[10] shown in cloumn 2 of Table I. The largest of these states are the simple proton particle states so that, to first order, the $^{116}Sn(\alpha, p)^{119}Sb$ reaction is similar to the $^{118}Sn(^3He, d)^{119}Sb$ reaction.[12]

The most interesting information to be gained from Table I comes from a comparison of the (α, p) data to the $(^6Li, 3n\gamma)$ data.[11] The states observed in the $(^6Li, 3n\gamma)$ experiment are believed to

TABLE I. Levels of ^{119}Sb (MeV).

(α,p) [a]	$(p,n\gamma)$ [b]	(^{6}Li,$3n\gamma$) [c]	J^π
0.000			$\frac{5}{2}^+$
0.266	0.2705		$\frac{7}{2}^+$
0.642	0.6439		$\frac{1}{2}^+$
0.700	0.6997		$\frac{3}{2}^+$
	0.971	0.971	$\frac{9}{2}^+$
	1.048		$\frac{7}{2}^+$
1.217	1.2127		$\frac{9}{2}^+$
	1.2496		$\frac{9}{2}^+$
	1.3273		
	1.3358		
	1.3389	1.341	$\frac{11}{2}^+$
1.366	1.3663		$\frac{11}{2}^-$
	1.4071		
	1.4138		
1.450			
	1.4674		
	1.4874		
	1.5448		
	1.6471		
1.660	1.6623		
	1.6757	1.676	$\frac{13}{2}^+$
	1.7217		
	1.728		
1.742	1.7496		
	1.8078		
1.829	1.821		
	1.876		
	1.887		
	1.9544		
1.975			
		2.038	$\frac{15}{2}^+$
	2.093		
2.121	2.118		
	2.123		
2.223	2.227		
2.298	2.291		
2.384			
		2.419	$\frac{17}{2}^+$
2.508			
2.624			
2.749			
3.778 ± 0.015			
3.830 ± 0.015			
4.020 ± 0.015			$(\frac{23}{2}^+,\frac{25}{2}^+)$
4.120 ± 0.015			$(\frac{19}{2}^+,\frac{21}{2}^+)$
4.210 ± 0.015			$(\frac{19}{2}^+,\frac{21}{2}^+)$

[a] This experiment. Errors on levels below 3 MeV are ±0.008 MeV.
[b] Reference 11.
[c] Reference 12.

be members of a $K^\pi=\frac{9}{2}^+$ rotational band built upon the $\frac{9}{2}^+$ state at 0.971 MeV. None of the states has been definitely observed in the (α,p) data presented here. This is consistent with the identification of these levels as belonging to rotations built upon a $(\pi g_{9/2})^{-1}$ hole structure. Due to the 50 keV resolution, the $\frac{13}{2}^+$ (1.676 MeV) member of this band cannot be clearly resolved from the peak at 1.660 MeV observed in this work. Nonetheless, the (α,p) angular distribution for the 1.660 MeV level is fit quite well by the empirical shape obtained from the known $\frac{7}{2}^+$ peak at 0.266 MeV, an indication that any population of the $\frac{13}{2}^+$ rotational state must be small. The observed shapes of the angular distributions for the levels in the region of the rotational $\frac{15}{2}^+$ (2.038 MeV) and $\frac{17}{2}^+$ (2.419 MeV) levels are also those from low spin states, thus precluding any significant population of the rotational levels. In fact, all the angular distributions for peaks below 3 MeV were found to be forward peaked, with shapes similar to the $\frac{1}{2}^+$, $\frac{3}{2}^+$, $\frac{5}{2}^+$, $\frac{7}{2}^+$, and $\frac{11}{2}^-$ angular distributions of the known particle states.

The angular distributions for the high spin candidates are found in Fig. 2. It can be seen by inspecting Fig. 2 that the high spin states are characterized by angular distributions that peak at large angles. Because the states of interest are 4 MeV in excitation energy, they ride on a background of low spin states that have forward peaked angular distributions. Consequently, the high spin states are obscured at small angles and are only visible near the maxima of their angular distributions.

III. DWBA CALCULATIONS

Because the (α,p) reaction has not previously been used to populate known high spin states in this region, J^π assignments for the high spin states cannot be made on the basis of an empirical comparison of angular distribution shapes. Therefore, it is necessary to rely on DWBA calculations to make the assignments. Recently, DWBA calculations for the three-nucleon transfer using cluster form factors and well-matched[13] optical potentials have enjoyed considerable success fitting $L=7$ and 9 transfers observed in the ^{40}Ca$(\alpha,p)^{43}$Sc (Ref. 7) reaction and the $L=8$ and 10 transfers seen in the ^{208}Pb$(p,\alpha)^{205}$Tl reaction.[8] This is the approach taken here also.

The DWBA calculations were performed with the code DWUCK.[14] The optical potentials were provided by Markham *et al.*,[15] who successfully fit transitions observed in the Te(p,α)Sb reactions at 35 MeV. These parameters, which meet the well-matching criteria of having identical real well geometrical parameters and a deep α potential, are given in Table II. The transferred "triton" was also bound in a well with the same geometry. The bound state well depth was allowed to vary to reproduce the proper binding energy. Typical depths were around 120 MeV, in accor-

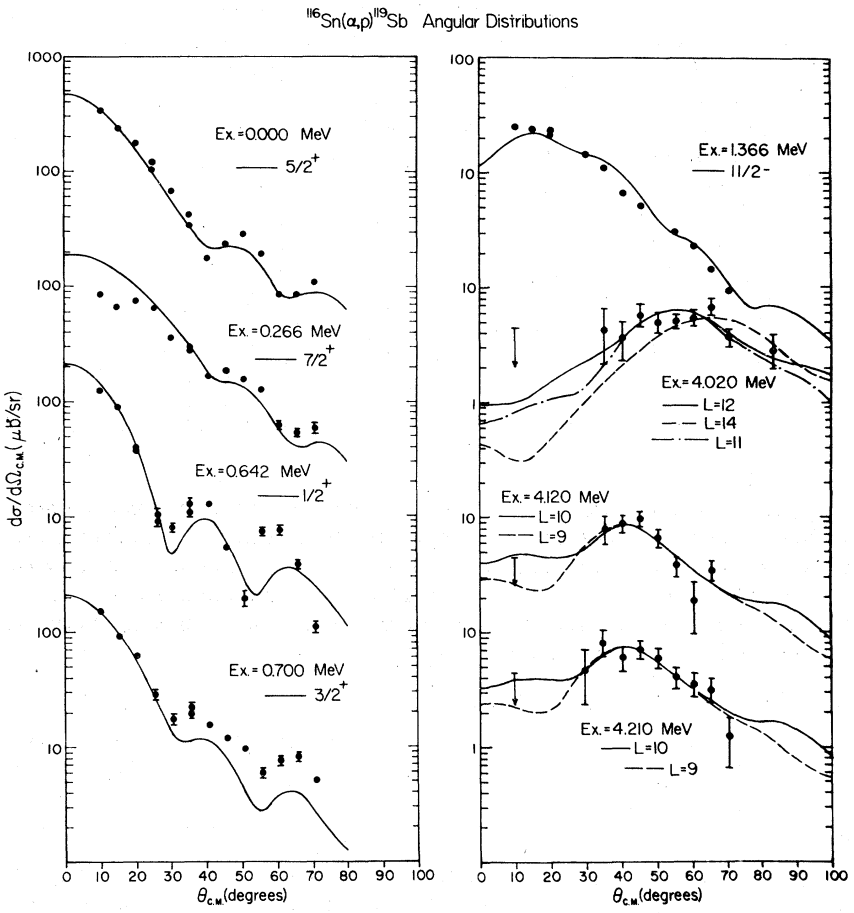

FIG. 2. Angular distributions for the high spin states and the strong single-particle states. The curves are the results of DWBA calculations using cluster form factors.

dance with the well-matching procedure. The predicted j transfer shapes compare favorably with those measured experimentally. However, the low spin states are fitted a little better if the diffuseness is decreased slightly as indicated in Table II. The fits are shown in Fig. 2, where the known particle states are included to demonstrate the quality of the fits.

The angular distributions for the 4.120 and 4.210 MeV states are reproduced equally well by $L=9$ and 10 curves. The $L=9$ and 10 predictions are sufficiently different from $L=8$ or 11 calculations to rule out these latter two choices. The angular distribution for the 4.020 MeV state is best fit by $L=11$ or 12 curves. Given the quality of the data an $L=14$ transfer cannot be excluded for this transition, although the angular momentum transfer is certainly greater than 10 $\hbar$.

Although the $L=9$ and 11 curves fit some of the data quite well (see Fig. 2), nuclear structure and microscopic reaction mechanism considerations make them unlikely assignments. A microscopic three-nucleon form factor is constructed by projecting the center-of-mass motion of three nucleons in an internal s state out of a product of three single-nucleon wave functions. This form

TABLE II. Optical parameters.

Channel	V (MeV)	r_0 (fm)	a_r (fm)	W (MeV)	r_i (fm)	a_i (fm)	V_{so} [a] (MeV)	r_{so} (fm)	a_{so} (fm)	W_D [a] (MeV)
α	−180.44	1.22	0.72	−41.85	1.32	0.80				
p	−46.87	1.22	0.72	−5.0	1.32	0.62	−24.8	1.06	0.68	19.88
Form factor	vary to fit BE	1.22	0.60							

[a] Includes factor of 4 used in DWUCK input (Ref. 14).

factor is generally created by one of two methods: Harmonic oscillator single-particle wave functions are transformed by a pair of Moshinsky transformations[16] or wave functions generated in a Woods-Saxon well are transformed by a generalization of the Bayman and Kallio method commonly used to compute two-nucleon form factors.[17] (See Ref. 6 for details and a list of references.)

If the harmonic oscillator approach is taken, the form factor may be written as

$$F^{LSJ}(R) = \sum_{\nu L_n} G_\nu^{LSJL_n}\, \phi_\nu^L(R) \cdots , \tag{1}$$

where

$$G_\nu^{LSJL_n} = \sum_{(n_i l_i j_i)} C^{LSJ}_{(n_i l_i j_i) L_n} \Delta \begin{bmatrix} l_1 & \frac{1}{2} & j_1 \\ l_2 & \frac{1}{2} & j_2 \\ L_n & 0 & L_n \end{bmatrix} \begin{bmatrix} l_n & 0 & L_n \\ l_3 & \frac{1}{2} & j_3 \\ L & \frac{1}{2} & J \end{bmatrix}$$

$$\times \sum_{\nu_{12}} \langle (N_{12} - \nu_{12}) 0 \nu_{12} L_n : L_n | n_1 l_1 n_2 l_2 : L_n \rangle_{11} \langle (N - \nu) 0 \nu L : L | \nu_{12} L_n n_3 l_3 : L \rangle_{21} \Omega(\alpha, \beta) \phi_\nu^L(R) \cdots . \tag{2}$$

(See Table III for a summary of the notation.)

The term $\Omega(\alpha, \beta)$ is an internal integral which, among other terms, is a function of the size parameter difference $(\beta - \alpha)$ raised to the number of internal nodes. If the size parameters of the target nucleus (β) and the α particle (α) are taken to be the same, a zero form factor results, unless the number of internal nodes is zero. Thus the sum over ν in Eq. (1) reduces to one term where ν is the maximum number of nodes. In this form Eq. (1) consists of a normalization factor and a cluster center-of-mass wave function. A cluster spectroscopic factor for a single configuration can be defined by

$$S_{L_n}^{LSJ} = \Delta \begin{bmatrix} l_1 & \frac{1}{2} & j_1 \\ l_2 & \frac{1}{2} & j_2 \\ L_n & 0 & L_n \end{bmatrix} \begin{bmatrix} L_n & 0 & L_n \\ l_3 & \frac{1}{2} & j_3 \\ L & \frac{1}{2} & J \end{bmatrix} \langle 00 N_{12} L_n : L_n | n_1 l_1 n_2 l_2 : L_n \rangle_{11} \langle 00 N L : L | N_{12} L_n n_3 l_3 : L \rangle_{21} \Omega(\alpha = \beta) \cdots . \tag{3}$$

The reaction cross section scales like $|S_{L_n}^{LSJ}|^2$. The odd L transfer values would require an $(h_{11/2})^3$ configuration. Thus we can compare the likelihood of observing an $L = 9$ transition to that of an $L = 10$ transition by examining the appropriate calculated $|S_{L_n}^{LSJ}|^2$ values. Table IV is a list of these $|S_{L_n}^{LSJ}|^2$ values. The largest single spectroscopic factor for an $L = 9$ transition is 38% of that expected for the $L = 10$ transitions. However, this percentage is only realized if there is a state with a pure $[\pi h_{11/2} \nu (h_{11/2})^2_4]_{19/2}$ wave function. In general a $\frac{19}{2}^-$ state in this limited basis will be a mixture of the four possible L_n values, so that the realistic spectroscopic factor should be calculated with the

TABLE III. Meaning of symbols used in text.

Symbol	Meaning
$F^{LSJ}(R)$	form factor.
$G_\nu^{LSJL_n}$	three-nucleon structure amplitude.
ν	number of nodes in the center-of-mass wave function.
L_n	the angular momentum of the two neutrons.
$\phi_\nu^L(R)$	the harmonic oscillator wave function for the center-of-mass motion.
$C^{LSJ}_{(n_i l_i j_i) L_n}$	coefficients for expanding the final state in terms of the target plus three nucleons with quantum numbers $\{n_i, l_i, j_i\}$.
Δ	normalization factor which expresses the effect of the Pauli principle.
[ ]	j-j coupling to l-s coupling transformation coefficients.
$\langle \vert \rangle_{ij}$	Moshinsky transformation coefficients for masses i and j.
ν_{12}	number of nodes in the center of mass motion of the two neutrons.
$\Omega(\alpha, \beta)$	the integral over the internal coordinates.
β, α	the sizes parameters of the target, α particle.
$S_{L_n}^{LSJ}$	cluster spectroscopic factor.

TABLE IV. Cluster spectroscopic factors.[a]

		$(h_{11/2})^3$		
		$L=9, J=\frac{17}{2}$		
L_n	4	6	8	10
$\lvert S\rvert^2$	0.015	0.025	0.031	0.032
		$L=9, J=\frac{19}{2}$		
L_n	4	6	8	10
$\lvert S\rvert^2$	0.380	0.147	0.080	0.038
		$[\pi s_{1/2}\nu(h_{11/2})^2_{10}]$		
		$L=10, J=\frac{19}{2}$		
L_n	10			
$\lvert S\rvert^2$	1.0			
		$L=10, J=\frac{21}{2}$		
$\lvert S\rvert^2$	1.0			

[a] Normalized so that $\lvert S\rvert^2=1.0$ for $\frac{21}{2}^+$.

coherent sum indicated in Eq. (1). This could either increase or decrease the probability of observing any one of the four $\frac{19}{2}^-$ states. In this instance, however, the spectroscopic amplitude for $L_n=4$ is so much larger than the other possible S values that mixing can only result in diluting the predicted $\frac{19}{2}^-$ strength. Therefore, it is reasonable to expect that the largest $L=9$ transfer has no more than $\frac{1}{3}$ the cross section of the $L=10$ transitions. Furthermore, it is much less likely that two $L=9$ transitions would be observed.

Table IV also demonstrates that the $\frac{19}{2}^+$ and $\frac{21}{2}^+$ transitions should occur with equal probability. This is further evidence for the $L=10$ assignments since the 4.120 and 4.210 MeV states have been observed with equal cross sections.

IV. RESIDUAL INTERACTION MATRIX ELEMENTS

In a standard shell model an inactive core such as ^{16}O, ^{40}Ca, or ^{208}Pb is chosen as a binding energy reference. If empirical shell model calculations are to be extended to more complicated nuclei, where perhaps only the protons or neutrons are closed, it is likely that the greatest success will be realized for the high spin states since they belong to a basis space with small dimensions, whereas the low spin basis state dimensions may be very large. One region where such calculations might be successful consists of the nuclei near tin where the $Z=50$ closure occurs. In this case it is not obvious what to do about a reference binding energy. Since the neutrons are in midshell, there is no natural boundary that makes any given stable Sn isotope special. The approach taken here was to determine the core according to a postulated wave function of the state in question. For example, the isomeric 8^- in the odd-odd Sb isotopes is postulated to be the stretched alignment of the $(\nu h_{11/2}\pi d_{5/2})$ configuration. Thus a ^{116}Sn core is appropriate for calculating the binding energy of the 8^- in ^{118}Sb, but the 8^- of ^{120}Sb requires ^{118}Sn as a core.

We have tested this model by calculating residual interaction matrix elements for a number of two-particle states and comparing the results with systematics given by Schiffer.[18] The $(\nu h_{11/2}\pi d_{5/2})$ multiplet was considered first because of the extensive work on ^{122}Sb that has been published quite recently.[19] An attempt is made in Ref. 19 to order the ^{122}Sb levels according to $n-p$ multiplets. Their assignment of the isomeric 8^- state to the $(\pi g_{7/2}\nu h_{11/2})$ multiplet is suspect, however, since the 9^- matrix element of this multiplet is expected to be the most attractive, thus requiring that there be a 9^- state below the 164 keV 8^- state. Since there is no known 9^- state below the 8^- level, it seems likely that this 8^- belongs to the $(\nu h_{11/2}\pi d_{5/2})$ multiplet. Upon making this assignment and accepting the rest of the assignments given in Ref. 19 for the $(\nu h_{11/2}\pi d_{5/2})$ multiplet, the matrix elements were found to be in reasonable agreement with the systematics shown in Fig. 8 of Ref. 18, with the exception of the 7^-. Closer examination of the level scheme given in Ref. 19 reveals a level at 703 keV with a $6,7^-$ assignment. If this level is assumed to be the 7^- that belongs to the $(\nu h_{11/2}\pi d_{5/2})$ configuration, the resulting matrix elements are in outstanding agreement with the particle-particle matrix element systematics, as shown in Table V. It should be noted that the results would not be noticeably different if the 5^- and 6^- assignments were reversed, and similarly for the 3^- and 4^- states.

The core dependence is tested by comparing the isomeric 8^- states of ^{116}Sb and ^{118}Sb. The matrix element calculated from the ^{118}Sb case is found to be -665 keV which differs from the ^{122}Sb case by only 13 keV (see Table III). On the other hand, the ^{116}Sb 8^- state yields a matrix element of -551 keV.

In order to perform three-particle calculations for the high spin states of ^{119}Sb, one must know the matrix elements for the high spin couplings of the $(\nu h_{11/2})^2$ configuration in ^{118}Sn. Both the 10^+ and 8^+ states of this configuration have been tentatively assigned. The matrix elements for these two cases are also given in Table V. Once again they are in reasonable agreement with particle-particle matrix element systematics in that they are repulsive. Since the analogous states are also known in ^{116}Sb we can again investigate the core dependence of the matrix elements. In this case the $(\nu h_{11/2})^2_{10,8}$ matrix elements are found

TABLE V. Residual interaction matrix elements.

Configuration	Core	Nucleus	Excitation (keV)	Matrix element (keV)	$E/\bar{E}$	$E/\bar{E}$ Ref. 18
$(\nu h_{11/2}\pi d_{5/2})_{8^-}$	^{120}Sn	^{122}Sb	164	−652	−1.54	−1.6
$(\nu h_{11/2}\pi d_{5/2})_{7^-}$	^{120}Sn	^{122}Sb	703	−108	−0.25	−0.25
$(\nu h_{11/2}\pi d_{5/2})_{6^-}$	^{120}Sn	^{122}Sb	414	−402	−0.95	−1.0
$(\nu h_{11/2}\pi d_{5/2})_{5^-}$	^{120}Sn	^{122}Sb	425	−391	−0.92	−0.75
$(\nu h_{11/2}\pi d_{5/2})_{4^-}$	^{120}Sn	^{122}Sb	311	−565	−1.20	−1.25
$(\nu h_{11/2}\pi d_{5/2})_{3^-}$	^{120}Sn	^{122}Sb	283	−535	−1.25	−1.5
$(\nu h_{11/2}\pi d_{5/2})_{8^-}$	^{116}Sn	^{118}Sb	212	−665	...	...
$(\nu h_{11/2}\pi d_{5/2})_{8^-}$	^{114}Sn	^{116}Sb	610	−551	...	...
$(\nu h_{11/2}\pi s_{1/2})_{5^-}$	^{116}Sn	^{119}Sb	a	−164	−0.81	−0.8
$(\nu h_{11/2}\pi s_{1/2})_{6^-}$	^{116}Sn	^{119}Sb	a	−233	−1.16	−1.2
$(\nu h_{11/2})^2_{10^+}$	^{116}Sn	^{118}Sn	3111	87	...	...
$(\nu h_{11/2})^2_{8^+}$	^{116}Sn	^{118}Sn	3055	31	...	...
$(\nu h_{11/2})^2_{10^+}$	^{114}Sn	^{116}Sn	3300	−162	...	...
$(\nu h_{11/2})^2_{8^+}$	^{114}Sn	^{116}Sn	3231	−231	...	...

[a] Calculated assuming the $\frac{19^+}{2}$ and $\frac{21^+}{2}$ states of ^{119}Sb are assigned as discussed in the text.

to be −162 and −231 keV, respectively. Again mass 116 yields a disconcerting result. The problems with the 8^- of ^{116}Sb and the 10^+ and 8^+ levels of ^{116}Sn can be attributed to the single-particle energy used for the $h_{11/2}$ neutron. If this energy, which enters into the 8^- calculation once and the 10^+ and 8^+ calculations twice, is decreased by about 125 keV, the matrix elements are found to be independent of the core. A deviation of this magnitude can easily be an effect of core polarization.

Since two $L=10$ transfers are observed in the ^{116}Sn$(\alpha,p)^{119}$Sb reaction, it is likely that they are the $\frac{19}{2}^+$ and $\frac{21}{2}^+$ states associated with the $[\nu(h_{11/2})^2_{10}\pi s_{1/2}]$ configuration. Assuming this to be the case, we get two binding energy equations, similar to the one given in the Introduction. These equations both contain a term which is the binding energy of the 10^+ level in ^{118}Sn, and two terms which contain the $(\nu h_{11/2}\pi s_{1/2})_{5^-}$ and $(\nu h_{11/2}\pi s_{1/2})_{6^-}$ matrix elements. Since the energy of the ^{118}Sn, 10^+ state is known, we can solve the simultaneous equations to obtain the $(\nu h_{11/2}\pi s_{1/2})_{5^-,6^-}$ matrix elements. The results are −219 keV (5^-) and −168 keV (6^-) if the 4.120 MeV state is assigned $\frac{19}{2}^+$ and the 4.210 MeV state is chosen at $\frac{21}{2}^+$. If the J^π assignments are reversed (4.120 MeV state assigned $\frac{21}{2}^+$) then the matrix elements are −164 keV (5^-) and −233 keV (6^-). Normalizing each matrix element E to the multiplet energy centroid $\bar{E}$ yields the values $((E/\bar{E})_{5^-},(E/\bar{E})_{6^-})=(-1.14,-0.88)$ and $(-0.81,-1.16)$ for the above choices. The second set is in excellent agreement with the values $(-0.8,-1.2)$ taken from Fig. 8 of Ref. 18 while the first set is not.

V. CONCLUSIONS

The ^{116}Sn$(\alpha,p)^{119}$Sb reaction has been successfully used to locate states in ^{119}Sb with probable orbital angular momenta of $10\hbar$ and $12\hbar$. Cluster model DWBA calculations have been used to identify the L transfer. The ambiguity of the $L=9$ and 10 fits to the data has been resolved with semimicroscopic reaction mechanism considerations. These calculations indicate that the $L=9$ transition strength is much less than that of the $L=10$ strength and that the $\frac{19}{2}^+$ and $\frac{21}{2}^+$ states should be populated equally. Two levels with equal cross section are observed which can be fit by $L=10$ transition shapes.

The intrinsic nature of these states is indicated by the following circumstantial evidence. First, no member of the previously identified $K^\pi=\frac{9}{2}^+$ rotational band was observed with any measurable strength. Furthermore, the systematics of this band in the lighter Sb isotopes suggest that the $\frac{19}{2}^+$ and $\frac{21}{2}^+$ states of that band are about 1 MeV below the states observed with the $L=10$ transfers in this work.

Secondly, explicitly assuming intrinsic wave functions with the configuration $[\pi s_{1/2}\nu(h_{11/2})^2_{10}]_{19/2,21/2}$

yields a prediction of equal population of the $\frac{19}{2}^+$ and $\frac{21}{2}^+$ states, which is borne out by the data.

Thirdly, simple one component shell model wave functions yield residual interaction matrix elements for the $(\pi s_{1/2}\nu h_{11/2})_{5^-,6^-}$ configurations that are consistent with previously documented matrix element systematics. The reliability of these matrix elements has been invistigated by calculating many matrix elements for states in this mass region assuming simple wave functions. These matrix elements also generally agree with systematics.

This work was supported in part by the U. S. Department of Energy.

[1]C. G. Linden, I. Bergstrom, J. Blomqvist, K. G. Renfelt, H. Weigolle, and K. Westerberg, Z. Phys. A277, 273 (1976).
[2]I. Bergstrom, J. Blomqvist, C. H. Herrlander, and C. G. Linden, Z. Phys. A278, 257 (1976).
[3]I. Bergstrom, B. Fant, C. J. Herrlander, K. Wilkstrom, and J. Blomqvist, Phys. Scripta 1, 243 (1970).
[4]I. Bergstrom, J. Blomqvist, C. J. Herrlander, K. Wilkstrom, and B. Fant, Phys. Scripta 10, 287 (1974).
[5]I. Bergstrom, C. J. Herrlander, P. Thieberger, and J. Blomqvist, Phys. Rev. 181, 1642 (1969).
[6]P. A. Smith, Ph.D. thesis, Michigan State University (unpublished).
[7]P. A. Smith and R. J. Peterson, Bull. Am. Phys. Soc. 22, 1008 (1977); (to be published).
[8]P. A. Smith, G. M. Crawley, R. G. Markham, and D. Weber, Phys. Rev. C 18, 2486 (1978).
[9]R. A. Emigh, Nucl. Instrum. Methods 156, 603 (1978).
[10]J. A. Carr, K. Shafer, R. A. Warner, W. D. McHarris, and W. H. Kelly, private communication.
[11]A. K. Gaigolas, R. E. Shroy, G. Schatz, and D. B. Fossan, Phys. Rev. Lett. 35, 555 (1975).
[12]M. Conjeaud, S. Harar, and Y. Cassagnou, Nucl. Phys. A117, 449 (1968).
[13]R. Stock, R. Bock, P. David, H. H. Duhm, and T. Tamura, Nucl. Phys. A104, 136 (1967).
[14]P. D. Kunz, private communication.
[15]R. G. Markham, R. K. Bhomik, P. A. Smith, J. A. Nolen, Jr., and M. A. M. Shahabuddin, Bull. Am. Phys. Soc. 21, 634 (1976).
[16]Y. F. Smirnov, Nucl. Phys. 27, 177 (1961).
[17]B. F. Bayman and A. Kallio, Phys. Rev. 156, 1121 (1967).
[18]J. P. Schiffer, in *Two Body Forces in Nuclei*, edited by S. M. Austin and G. M. Crawley (Plenum, New York, 1972), p. 205.
[19]V. L. Alexeev *et al.*, Nucl. Phys. A297, 373 (1978).